Journal of Applied Polymer Science

Polyurethane Foams Made from Liquefied Bark-Based Polyols

Jason D'Souza,[1] Rafael Camargo,[2] Ning Yan[1]
[1]Faculty of Forestry, University of Toronto, Ontario M5S 3B3, Canada
[2]Huntsman Advanced Technology Center, Huntsman International LLC, The Woodlands, Texas 77381
Correspondence to: N. Yan (E-mail: ning.yan@utoronto.ca)

ABSTRACT: Liquefaction is known to be an effective method for converting biomass into a polyol. However, the relationships between bark liquefaction conditions and properties of the resulting foams are unclear. In this study, polyurethane foams (PUF) were made using bark-based polyols obtained through liquefaction reactions of bark at two different temperatures (90 and 130°C). Through systematic characterization of the PUFs the influence of the liquefied bark and liquefaction conditions on foam properties could be observed. The bark-based foams had similar foaming kinetics, thermal stability, and glass transition temperatures compared with the PEG-based control foam. The bark-based PUF from the polyol obtained at the higher liquefaction temperature showed comparable specific compressive strength to the PEG-based control foam. Lastly, both bark foams exhibited a high amount of open-cell content, with the foam made from the lower temperature liquefied polyol having poor cell morphology. This deviation from the controls in the open-cell content may explain the lower modulus values observed in the bark PUFs due to the lack of cell membrane elastic stretching as a strengthening mechanism. These results demonstrated the influence of the bark liquefaction conditions on foam properties, thereby providing a better fundamental understanding for the practical application of bark-based PUFs. © 2014 Wiley Periodicals, Inc. J. Appl. Polym. Sci. **2014**, *131*, 40599.

KEYWORDS: biopolymers and renewable polymers; cellulose and other wood products; foams; morphology; polyurethanes

Received 25 July 2013; accepted 14 February 2014
DOI: 10.1002/app.40599

INTRODUCTION

Bark is a renewable raw material that has garnered much interest for the production of precursor chemicals for the synthesis of phenol-formaldehyde adhesives,[1] furfuryl- formaldehyde foams,[2–4] and polyurethane foams (PUFs).[5–8] PUFs are known most notably for their versatility enabling their utilization as low-density flexible foams in the automotive industry and as insulation in appliances, homes, and commercial buildings. PUFs are made through an addition reaction of an isocyanate with an active hydrogen group, typically a hydroxyl or water. Polyether or polyester polymers with hydroxyl end groups are commonly used, however these are mostly derived from petroleum based resources.

Significant efforts have been made to derive polyols through the liquefaction of lignocellulosic biomass through glycolysis with an acid catalyst. This method digests the biomass into a low viscosity liquid polyol and has been used to produce polyols from a wide variety of biomass materials including bamboo,[9] lignin,[10] wood meal,[11,12] soybean,[13] and wheat[14] straws, sugar cane bagasse,[15] and bark.[7,8,16]

Bark is an underutilized source of biomass material suitable for industrial applications because of its abundant availability as a low-value mill residue. Lodgepole pine (*Pinus Contorta*) bark was used in this work. The thickness of this bark relative to the tree trunk diameter was found to be 6.9%.[17] This large volume of bark is mostly burnt in boilers, despite it being a rich source of polyphenolic compounds like condensed tannins at up to 30% of bark's weight.[18] The potential utility of these polyphenolic compounds stems from their high level of hydroxyl functionality; their ease of extraction compared to recalcitrant biopolymers like lignin and cellulose; and their aromaticity that can potentially impart thermal stability to their resultant PUFs.[19,20]

Bark-based PUFs were initially made through mechanically mixing bark or tannin extracts into polyols.[5,6] Furthermore, the work done on liquefied bark has focused on the properties of flexible PUFs[7,16] or on foams produced from harsh liquefaction conditions above 200°C.[8] Even though higher liquefaction temperatures can produce a higher yield, the resulting polyols will also have a higher viscosity with more degradation products.

In previous work, lodgepole pine bark was liquefied at mild temperatures of 90 and 130°C to produce two polyols: P90 and P130.[21] Both polyols primarily consist of compounds derived from extractives and polysaccharides. Carbon NMR spectra

Table I. Characteristics of Bark-Based Polyols to Controls

Polyol type	Liquefaction yield (%)	Bark content in polyol[a] (%)	OHV (mg KOH/g)	Functionality	Viscosity (cP)
PPG-G	–	–	429[b]	2.34[b]	142
PEG-G	–	–	435[b]	2.33[b]	155
P90	21	13.5[a]	429+/−1.2	NA	970
P130	28	12.3[a]	311+/−21.1	NA	717

[a] Values were calculated based on the liquefaction yield and the amount of PEG and glycerol used.
[b] Value was calculated based on 9 : 1 weight ratio and chemical structure.

showed that the P90 polyol contains some sugars and aromatic carbons. In contrast, the P130 polyol has sugar degradation products like levulinate esters and without detectable aromatic carbons. Regarding molecular weight, the P90 polyol has a large fraction of small molecular weight compounds lower than 600 Da. Additionally, from a ^{31}P-NMR method, both polyols only consist of aliphatic alcohols. Liquefaction produced a polyol with only aliphatic hydroxyls by grafting glycols onto phenolic structures through condensation reactions.[22] This is an advantageous feature since phenolics tend to produce unstable polyurethanes. The stability of a urethane linkage is related to the equilibrium between polymerization and depolymerization of a polyol and an isocyanate. Phenols react very slowly with isocyanate to produce unstable urethane linkages, while aliphatic alcohols react rapidly to yield thermally stable linkages.[20] This modification of bark is one advantage of liquefaction over simple thermomechanical mixing. The previous study has shown that bark polyols feature a hydroxyl value, hydroxyl type, and viscosity consistent with typical industrial polyols for making rigid PUFs.

What remains unknown is how the presence of bark compounds with unknown functionality and a broad molecular weight profile will impact foam characteristics like the foaming kinetics, the morphology, and the polymeric nature of the polyurethane polymer. In this study, the aforementioned polyols P90 and P130 were used to make bark-based PUFs named B90 and B130. These foams were contrasted to two controls designated PEG-G and PPG-G. The first is a polyethylene glycol (PEG) and glycerol blend that is similar in composition to the liquefaction solvent used to produce the bark polyols. The latter is a blend of polypropylene glycol-glycerol. Most liquefaction reactions are done in PEG and therefore a PEG polyol is an ideal control since the glycol structure, functionality, hydroxyl value, and viscosity will be similar to the liquefied polyol. However, commercial PUFs are predominantly based upon propoxylated structures. By using PPG as an additional control, the secondary hydroxyl content will be consistent with the hydroxyl type of commercial polyols. Finally, the diversity in formulations (amount and type of surfactants, catalysts, blowing agents; isocyanate type and index) makes comparisons to the literature difficult and therefore controls provide a useful alternative.

The goals of this study are two-fold. First, by comparing the bark-based foams to controls the effect of the bark content on foam properties can be examined. Second, the effect of the liquefaction temperature on properties of bark-based PUFs can be studied. Understanding the effect of bark content and the liquefaction conditions on foam properties is essential to determining the applicability of liquefaction as a process for the conversion of bark into a polyol.

EXPERIMENTAL

Materials

PEG with a molecular weight of 400 Da was purchased from Fisher Scientific. Glycerol, sulfuric acid, xylene, sodium hydroxide, dioxane, toluene, and pyridine were purchased from Caledon Laboratories. Imidazole, polypropylene glycol 425 and phthalic anhydride were purchased from Sigma Aldrich. All chemicals were used as received without further purification. Mountain pine beetle infested lodgepole pine (*Pinus Contorta*) bark was supplied by FPInnovations. It was ground into a powder using a Wiley mill and then passed through a 70 mesh sieve (0.251 mm). The powder was then dewaxed through a soxhlet extraction with hexanes for 4 h, after which it was dried in an oven overnight. RUBINATE® M polymeric MDI (pMDI) and two amine catalysts: *N,N*-dimethylcyclohexylamine (DMCHA) and pentamethyldiethylenetriamine (PMDETA; from the JEFFCAT® catalyst product line) were supplied by Huntsman. The surfactant DABCO DC5604 was supplied by Air Products.

Liquefaction

The liquefaction method has been reproduced here for convenience; however, the details of the characterization were previously reported.[21] Liquefactions were conducted at 90 and 130°C to produce bark-based polyols, P90, and P130. PEG (37.5, 30 g), glycerol (1.99, 1.59 g), sulfuric acid (1.99, 0.80 g), bark (37.5, 15 g), and a cosolvent (water-200, xylene-30 mL) were added to a flask fitted with a condenser. The flask was then heated for 1 h at the respective temperature under a nitrogen environment. Next, the solution was diluted with a dioxane-water (8 : 2) solution (600 mL), and then neutralized using a sodium hydroxide solution. The solutions were then centrifuged at 1500 RPM for 15 min, filtered, and washed with dioxane-water (8 : 2). The water and dioxane were then removed through rotary evaporation for a sufficient period to ensure maximal removal of water.

Polyol Characteristics

The details of the characterization were previously reported elsewhere,[21] but are summarized in Table I. The PEG-G and PPG-G polyols are a 9 : 1 blend by weight of glycol and glycerol. The bark polyols were produced using a 9 : 1 blend of PEG-400 and glycerol as a liquefaction solvent. Therefore, control samples

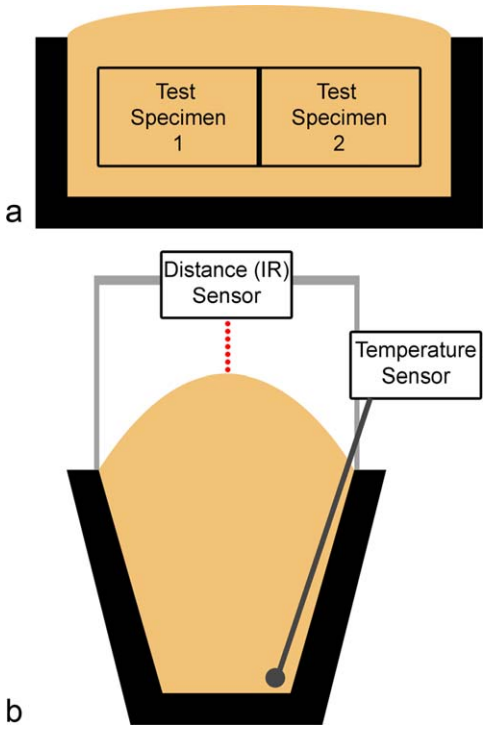

Figure 1. A schematic illustrating the (a) foam bun and sampling location and (b) the experimental set-up for measuring temperature and foam expansion within a cup. [Color figure can be viewed in the online issue, which is available at wileyonlinelibrary.com.]

and bark polyols both have similar glycerol content to facilitate a more meaningful comparison.

Formulation and Foaming

Each bun and cup foam required 22 g and 5 g of polyol, respectively. Relative to the weight of the polyol, 0.17% PMDETA, 0.83% DMCHA, 4% surfactant, and 5% water (as the blowing agent) were stirred together with the polyol, followed by sonication for 5 min.

Bun: The polyol solution was poured into a cup, and the calculated amount of pMDI was then added while on a scale to ensure an isocyanate index of ~1.1. The cup contents were mixed at high speed using an overhead mixer for 10 s, poured into a mold, and allowed to foam and polymerize. The samples were kept overnight at room temperature to cure before demolding. As depicted below in Figure 1(b) the sides of the foams were cut away, so that all samples were prepared from the inner core of the foam. Furthermore, samples were taken from a single plane to ensure any variation of properties along the rise direction would be similar in all samples.

Foaming Kinetics

The foaming kinetics were based upon measurements taken during foaming within a cup as depicted in Figure 1(b). The temperature and height were measured using a custom-made device consisting of an Arduino Duemilanove programmable microcontroller circuit board, a 10 k thermistor as a temperature sensor, and an infra-red distance sensor (Sharp GP2D120). After mixing for 10 s, the height sensor was clamped above the cup, and the thermistor cable was immersed into the foaming polymer; this point was considered the starting point or time zero of the analysis.

Polymer Characterization

Attenuated total reflection spectroscopy (ATR) was performed on samples prepared from bun-type foams. They were compressed using a press prior to analysis on a Bruker Tensor 27 FTIR spectrometer. Forty scans were taken for each sample with a resolution of 4 cm^{-1}. Thermogravimetric analysis (TGA) was done on a TA instruments Q50 TGA at a heating rate of 10°C/min under nitrogen. Glass transition values were obtained from an Anton Paar MCR-301 Rheometer using torsion clamps at a strain amplitude of 0.5% and a temperature ramp of 3°C/min from 25 to 200°C on rectangular bars with approximate dimensions of 50 × 10 × 5 mm. The glass transition value was determined from the peak of the tan delta plots. The degree of swelling and soluble fraction were determined based on a procedure from the literature.[23] Values were reported as an average of three measurements.

Foam Characterization

The closed-cell content, C_v, was determined using an Ultrapycnometer 1000 by Quantachrome Instruments using nitrogen gas. The closed-cell content was determined using the following set of equations:

$$O_v = [(V - V_{SPEC})/V] \times 100$$
$$W_v = [m/(\rho_{SOLID} \times V)] \times 100$$
$$C_v = 100 - O_v - W_v$$

where O_v is the percentage of open-cell content, V is the geometric volume as determined by calipers (g/cm^3), V_{SPEC} is the enclosed volume inaccessible to the inert gas obtained from the pycnometer, W_v is the percentage of volume occupied by cell walls, m is the mass of the specimen (g), ρ_{SOLID} is the density of solid polyurethane obtained from pycnometry measurements of a ground PUF (g/cm^3), and C_v is the percentage of closed-cell content. Samples were ~2 × 2 × 1 cm^3 and the value reported was an average of four samples. The cell morphology was studied using a stereo AMScope optical microscope using an AMScope MT1000 camera. Images were edited in ImageJ to add a scale bar and in Photoshop CS2 to desaturate and enhance contrast in the images. The foam density reported is based upon the bulk density of the bun-foam. The bun was cut into four rectangular prisms, each sample's volume and mass were measured, and the reported value is the average of the four samples.

Compression testing was done on an Instron tensile tester using compression clamps at a cross-head speed of 2.5 mm/min. Samples were cut from the bun foams into rectangular prisms of ~5 × 5 × 3 cm^3, compressed in the rise direction, and was done in triplicate.

RESULTS AND DISCUSSION

Foaming Kinetics

Studies on the kinetics of polyurethane reactions have been traditionally studied by ATR/FTIR,[24,25] the adiabatic temperature profile,[26] and by novel methods looking at changes in

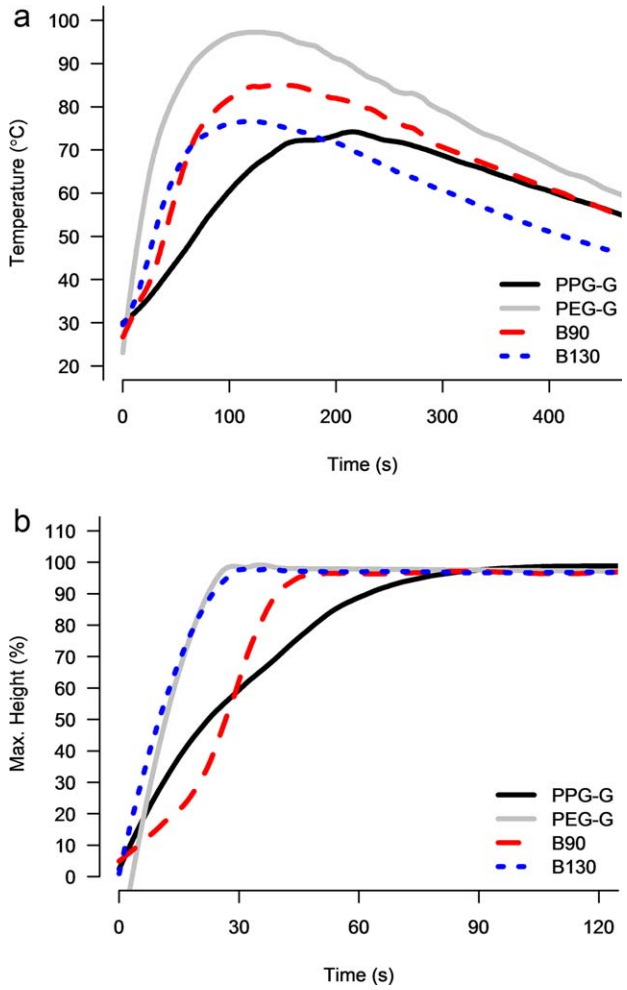

Figure 2. Foaming kinetics (a) showing the change in temperature during the foaming reaction and (b) showing the foaming rate (time to reach the maximum height) versus time. [Color figure can be viewed in the online issue, which is available at wileyonlinelibrary.com.]

resistivity.[27] However, the foaming kinetics of the PUFs made from liquefied polyols have not been examined to the same extent. In this work, the foaming rate and the temperature profile were used to make inferences about the reactivity of the polyols and the morphology.

Generally, isocyanate reacts fastest with primary hydroxyls and water, followed by secondary hydroxyls. The use of catalysts can further intensify these differences in reaction rates.[28,29] Therefore, a polyol with a greater concentration of primary hydroxyls will exhibit a greater mismatch between the blowing and gelling reactions, that will ultimately impact the morphology. Rapid foaming may be deleterious to foam properties if proper mixing is not achieved.

The first observable trend is that a greater concentration of primary alcohols produces a sharper exotherm as evident from the increased rate of temperature change and the maximum temperature attained. The graph in Figure 2(a) and data in Table II shows that the PEG-based foams (PEG-G, B90, and B130) exhibited the most rapid increases in temperature upon initiation of the foaming reaction. The main constituent of these foams is PEG-400 with two primary hydroxyl groups. In contrast the PPG-based foam consists of polypropylene glycol 425 with two secondary hydroxyls. The temperature profile of the PPG-G foam was noticeably delayed and reached a lower maximum temperature. The P90 polyol contains some secondary hydroxyls,[21] due to the presence of sugars, and had its temperature maxima occur later than PEG-G, but earlier than PPG-G. This intermediate curing behavior of B90 is clearer in Table II. B130 and PEG-G consist primarily of primary hydroxyls and both have similar profiles for their rate of expansion. Therefore, if liquefaction is done at low temperatures to preserve sugars, the resultant foams will have a greater amount of secondary hydroxyls, and foaming behavior will more closely resemble the behavior of a PPG-based foam. Since liquefied bark can contain a variety of hydroxyls, it is important to know the type and quantity since these results showed that the foaming kinetics can be impacted.

Another observation was that B130 has a lower hydroxyl value (311 mg KOH/g) compared with B90 and PEG-G (429, 435 mg KOH/g) that produced a lower maximum temperature. Therefore, all though B130 had a similar expansion profile to PEG-G [Figure 2(b)], the lower OHV of the polyol produced a milder exotherm, as there were less OH groups to undergo the exothermic reaction with isocyanate. In summary, mild liquefaction conditions of bark produced polyol reactivity intermediate to PEG-G and PPG-G control samples.

It should be noted that since foaming was done within a cup, heat loss occurred through the cup to the surrounding environment and via the heating and the evaporation of water to steam. Despite not being an adiabatic system, trends were still observed regarding the effects of hydroxyl type and the hydroxyl value on the foaming behavior.

Functional Groups

The polyurethane polymer structure was studied by analyzing its functional groups using attenuated total reflectance spectroscopy (ATR). The ATR spectra of the four foams are shown in Figure 3. All the foams have peaks that correspond to functionalities found in ureas and urethanes: a broad N—H peak at 3300 cm^{-1}, C—H peak at 2900 cm^{-1}, carbonyl peaks from 1650–1750 cm^{-1}, an aromatic ring stretch at 1580–1615 cm^{-1}, peaks from 1190 to 1130 cm^{-1} are characteristic of a C—N stretch of an aromatic secondary amine,[30] and the urethane linkage at ~1200 cm^{-1}.[31] PPG-G, B90, and B130 show a peak for unreacted isocyanate at 2275 cm^{-1}, despite a relatively low isocyanate index of 1.1. In addition to the formation of urea and urethane linkages, isocyanate can also undergo dimerization reactions to produce carboimides, as well as a trimerization reaction to produce an isocyanurate ring. Carboimides have a peak at 2140 cm^{-1} and can be observed as a small shoulder in B130, and small peaks in PPG-G and PEG-G. All four foams showed a peak at 1415 cm^{-1} that is indicative of an isocyanurate ring.[31] Isocyanurate rings increase the cross-linking density and are also stable at high temperatures. Catalysts were used to promote the gelling (urethane linkage) and blowing (urea linkage) reactions. However, these catalysts are also known to have

Table II. Parameters Used to Assess the Foaming Kinetics

	Maximum temperature (°C)	Time of maximum temperature (s)	Rate of temperature change dT/dt (°C/min)[a]	Time to maximum height (s)
PPG-G	74	210	21	88
PEG-G	97	125	47	25
B90	85	142	36	45
B130	77	119	39	28

[a] This value is the rate at which the foam reaches its maximum temperature chemical characteristics.

some activity at promoting isocyanurate formation.[25] In summary, the ATR results showed that the bark polyols reacted with isocyanate, leaving only a small residual NCO peak, and produced a mixture of urea and urethane linkages, consistent with a typical PUF.

Thermal Stability

Thermogravimetric analysis under an inert environment can provide insight into the composition through differences in the thermal stability of chemical bonds. The thermal decomposition of polyurethanes is a combination of random-chain scission, chain-end unzipping, and crosslinking.[20] From the literature, the urethane (200°C) and urea (250°C) linkages are the first to break and depolymerize back into free isocyanate and the alcohol. This is followed by degradation of the polyether polyols, and finally isocyanate past 600°C.[32]

In the TGA graphs in Figure 4(a), it can be seen that most of the weight loss occurred between 250 and 450°C. After this point the weight loss was minimal as the structures were now heavily crosslinked and resistant to degradation. It was expected for B130 to have the lowest residue amount since it had the lowest hydroxyl value and correspondingly the lowest weight fraction of thermally stable aromatic rings from the MDI structure. Instead, both bark foams showed higher amounts of char formation than the control foams. One possible explanation may be that the large molecular weight and aromatic structure of bark extractives lend themselves to char formation more easily than a polyether polyol.

In the D-TGA graphs in Figure 4(b), it can be seen that B90 began to degrade earlier than the other foams at around 200°C. This may be attributed to the decomposition of sugars from the P90 polyol.[33] After this initial degradation, the urethane linkage depolymerized to produce free isocyanate and polyol.[34] From the DTG graphs PEG-based polyols degraded throughout the temperature range of 250–400°C and resulted in large mass losses, with one large degradation maxima at 320°C, followed by a significantly smaller peak at 400°C. In contrast, PPG-G had degradation maxima at 285 and 365°C. These two peaks indicated differences may exist in phase behavior between the PPG-PUF and the PEG-based PUFs. Previous research has

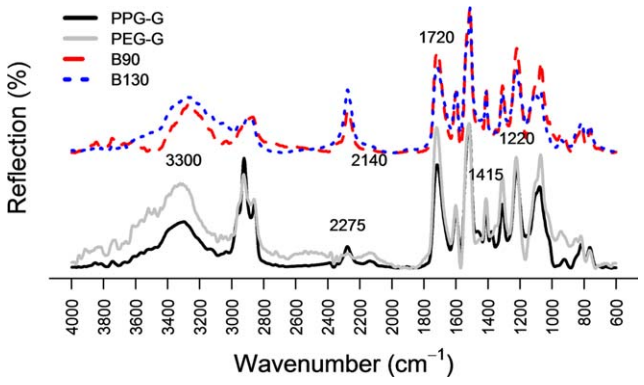

Figure 3. ATR Spectra of control foams PPG-G and PEG-G, and the bark-based foams B90 and B130. [Color figure can be viewed in the online issue, which is available at wileyonlinelibrary.com.]

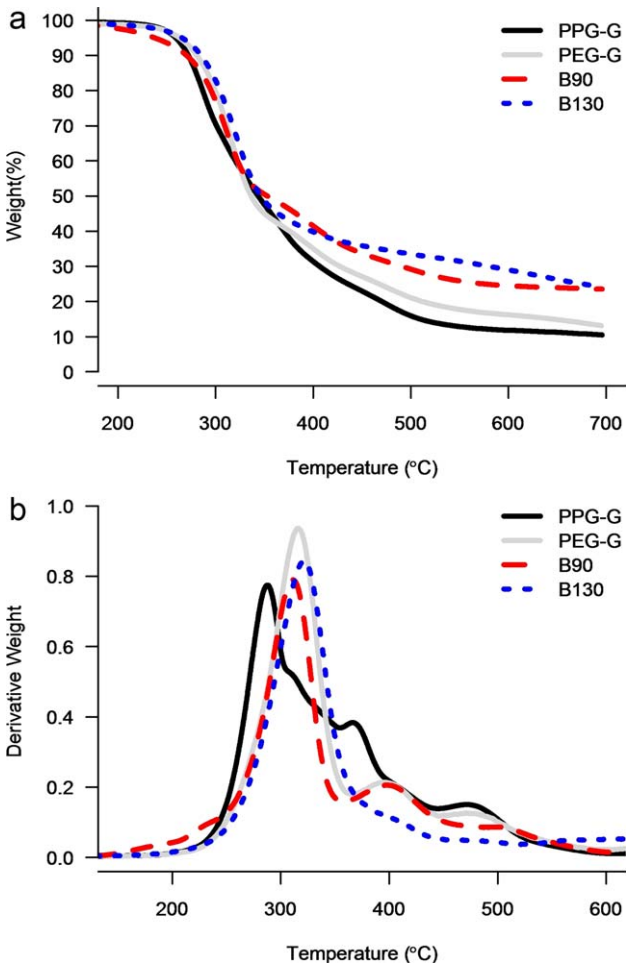

Figure 4. (a) TGA and (b) differential-TGA of control foams PPG-G and PEG-G versus bark-based foams B90 and B130; both under nitrogen. [Color figure can be viewed in the online issue, which is available at wileyonlinelibrary.com.]

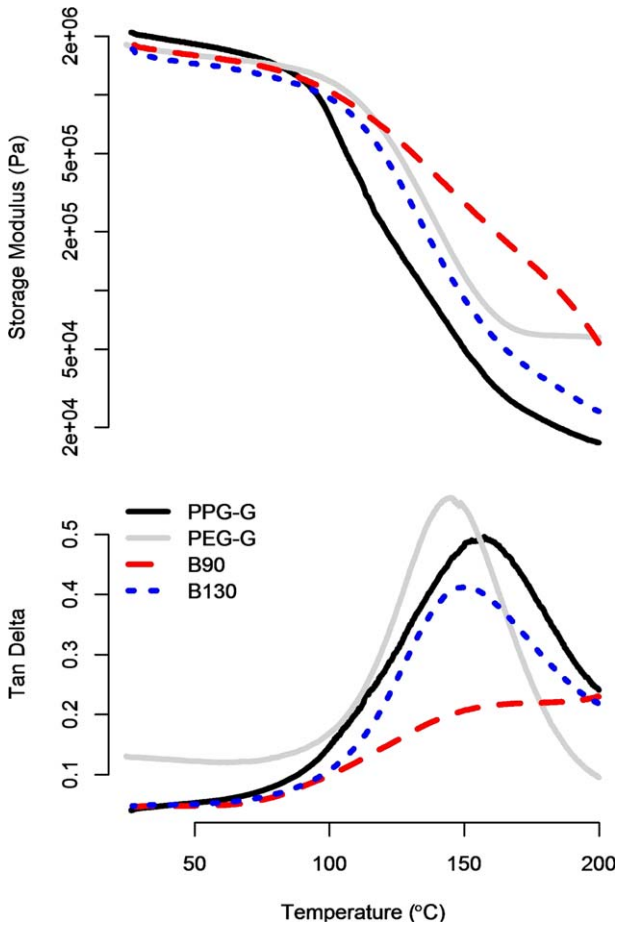

Figure 5. Storage modulus and tan delta plots, showing the glass transition temperatures of control (PEG-G and PPG-G) and bark (B90 and B130) PUFs. [Color figure can be viewed in the online issue, which is available at wileyonlinelibrary.com.]

shown that in an inert environment PEG-based polyurethanes are more thermally stable due a mutual stabilizing effect caused by extensive amounts of interurethane hydrogen bonding between intermixed hard and soft segment phases.[35] In contrast, PPG prevents miscibility of the phases. Without a mutual stabilizing effect, the PPG polyol degraded at lower temperatures than the PEG system.

Under an inert environment, these results showed that the PEG structure of the polyols produced more thermally stable PU polymers compared with a PPG-PUF. This has been described as a shielding effect due to mixed hard and soft segments. It can be seen that the inclusion of bark did not significantly impact the degradation behavior, other than increasing the amount of char formation, visible in Figure 4(a).

Network Formation and Crosslinking Behavior

The crosslinking behavior was studied indirectly via determination of the glass-transition temperature by dynamic mechanical rheometry, a solvent swelling test, and the soluble fraction. Determination of the glass transition temperature, T_g, provides insight into the observed mechanical properties through the effect of molecular weight, aromatic content, and crosslinking density on chain mobility. From the plot of the storage modulus of the four foams in Figure 5(a) it was evident that PPG-G had the steepest decline in the storage modulus, whereas the PEG foams had a delayed onset of storage modulus decay. This indicated a difference in the phase morphology may have existed. PEG-based PUFs tend to have increased miscibility between hard and soft segments,[35] which could have delayed the decrease in storage modulus. Focusing on just the PEG-based foams, the storage modulus behavior at room temperature for the bark foams was similar to PEG-G, but differed at elevated temperatures. B90 had its storage modulus decay the slowest, followed by the PEG-G foam, and lastly B130. These differences may be explained by a difference in the molecular weight between crosslinks, M_c, with a small M_c indicating a very rigid polymer. B90 has a large fraction of low molecular weight compounds that could have greatly reduced the M_c, despite the fact that it has a similar hydroxyl value to PEG-G. B130 however has the lowest hydroxyl value of the three, and therefore its M_c was expected to be the highest, and have the lowest storage modulus. Another observation was that only the PEG-G foam showed a clear rubbery plateau in its plot of storage modulus. This indicated a cohesive network with extensive curing. The high temperature of 97 °C observed in the foaming kinetics data in Table II could have prevented any vitrification from occurring. In contrast, the bark foams and PPG-G that had lower temperature exotherms have not exhibited a rubbery plateau and therefore may not have cured completely or have a more fragmented network. Therefore, it would appear that phase behavior, polyol molecular weight, and curing temperature may all have had an impact on the thermomechanical properties of the PUFs.

The peak of the tan delta graph in Figure 5(b) was used to determine the glass transition temperature. All four foams have a glass transition temperature within the range of 145–160°C. The PPG-G foam had the highest at 157°C, while PEG-G (145°C) and B130 (151°C) were slightly lower. The B90 foam did not exhibit a clear peak, but rather a slope change that occurred at ~151°C. The lack of a clear peak indicated that the B90 foam may have had a very broad range of molecular weight chains. The glass transition of B130 was within a few degrees of PEG-G, but interestingly the intensity of the tan delta peak was significantly less. Since tan delta is the ratio of the loss modulus to the storage modulus, a less intense tan delta peaks implies that a foam exhibits greater elastic behavior and restricted viscous flow. Increased functionality results in less intense tan delta peaks and increased glass transition temperatures.[36] This result suggests that B130 has a high functionality.

To conclude, bark content was observed to alter the thermomechanical properties of the PUF relative to the PEG-G sample. The high fraction of low molecular weight compounds in B90 produced a high storage modulus value at elevated temperatures, possibly due to a short M_c. However, a higher liquefaction temperature produced a more uniform polyol, and the corresponding foam B130 exhibited a clear glass transition temperature that was more consistent with the control samples.

The degree of swelling can indirectly assess the degree of crosslinking. Polymers that are heavily crosslinked do not expand as

Table III. Swelling and Soluble Fraction Data of the Control and Bark-Based PUFs

	PPG-G	PEG-G	B90	B130
Degree of swelling	1.23 ± 0.00	1.10 ± 0.01	1.44 ± 0.06	1.22 ± 0.03
Soluble fraction (%)	0.14 ± 0.23	0.53 ± 0.15	1.70 ± 0.21	1.47 ± 0.16

much due to a limited volume for solvent absorption. It can be seen from Table III that B90 appeared to swell the most, while B130 was similar to the control PUFs. By assessing the soluble fraction, B130 and to a greater extent B90, have polymer chains that have not been fully incorporated into the PUF network. Degraded bark components can have low functionality or perhaps none at all and can be leached easily from a PUF. These soluble fraction values were quite low with some contribution likely originating from leached catalyst and surfactant. Control samples contain the same amount of catalyst and surfactant, but may exhibit differences in solvent permeability that arose from the primarily open-celled bark foams as shown in Table IV. It should be noted that B130 showed a lower degree of swelling and soluble fraction than B90. The P90 polyol used to make the B90-PUF was shown to have contained a large fraction of low-molecular weight compounds compared with the P130 polyol used to make B130.[21] Removal of these low-molecular weight compounds from both polyols may be one method to improve the characteristics of bark-based PUFs as these compounds appeared to hinder the formation of a cohesive polymer network.

Morphology of the PUFs

The morphology of PUFs are known to correlate with many material properties, although thorough characterization of the morphology through microscopy is rarely done because it is often plagued by complexities associated with getting reproducible data and selection of appropriate methods.[37] Nonetheless, the optical micrographs in Figure 6 qualitatively showed that both controls (PPG-G and PEG-G) and B130 had the most uniform periodic cellular structure, whereas greater heterogeneity was observed for B90. All foams had some large pores indicating the coalescence of cells, but B90 appeared to have these defects at a greater frequency. Furthermore, the optical micrographs in Figure 6(e–h) show that the cellular structure was less defined in the bark foams, especially B90. Conversely, the cell structures of PPG-G and PEG-G in Figure 6(a–d) had sharper boundaries. This result implied that the bark polyols, especially the B90 polyol, did not form a stable network quick enough to preserve a cell structure, but rather underwent Ostwald ripening.

Aside from microscopy, the morphology can also be probed through characterization of the closed-cell content. This is an important characteristic of cellular materials due to its influence on heat transfer and the cell membrane's role in elastic stretching. It can be seen from Table IV that both bark-based foams had low values for closed-cell content compared with the control foams. Since the curing profiles of the bark foams were intermediate to both controls this was likely not due to the kinetics of foaming. Also, the bark polyols had a higher viscosity, so it was expected for them to have thicker membranes. Therefore, the low values for the closed-cell content could have originated from low-functionality compounds in the bark polyols. These compounds could have ruptured membranes by plasticizing them and prevented a cohesive polymer network from being formed in the membrane, and thus resulted in greater amounts of polymer drainage from the film. Or the compounds could have also acted as an antifoaming agent by reducing surface tension.[38] Optimization of both surfactant and catalysts may help to narrow this gap since the reactivity and the surface energy of bark polyols could differ from the controls. However, removal of low molecular weight compounds (likely with low functionality) may lead to remedying the low amount of closed cells.

Lastly, the foams were compared in the rise and transverse directions and it can be observed that the cells were stretched along the rise direction in all the foams, but B130 appeared to have been the least anisotropic foam with the least amount of elongation. Cell heterogeneity varied along the rise direction and as result this could have been an artifact associated with sample selection and foam preparation within a cup. The cause of anisotropy is generally due to the cells expanding in the least constrained direction, the rise direction.

Mechanical Properties

To understand the compressive behavior of PUFs it is important to begin with a discussion of the modulus and density, these values are shown in Table IV. The densities of the foams are

Table IV. Comparison of the Closed-Cell Content, Density, and Mechanical Properties of Bark-Based PUFs to Controls

Foam	Closed-cell content (%)	Density (kg/m^3)	Elastic modulus (MPa)	Compression strength 10% (kPa)	Compression strength 25% (kPa)	Normalized strength $\sigma_{10}/\rho^{3/2}$ [kPa/(kg/m^3)$^{3/2}$]
PPG-G	75.2 ± 0.8	34.9 ± 0.8	3.3 ± 0.1	194 ± 9.3	172 ± 12.1	0.94 ± 0.03
PEG-G	72.6 ± 2.2	35.5 ± 0.8	3.9 ± 0.7	162 ± 25.2	203 ± 19.1	0.61 ± 0.06
B90	1.4 ± 1.0	34.6 ± 1.5	1.1 ± 0.1	73 ± 8.5	85 ± 9.4	0.36 ± 0.02
B130	3.4 ± 1.4	28.8 ± 1.4	1.7 ± 0.1	100 ± 17.5	119 ± 1	0.65 ± 0.07

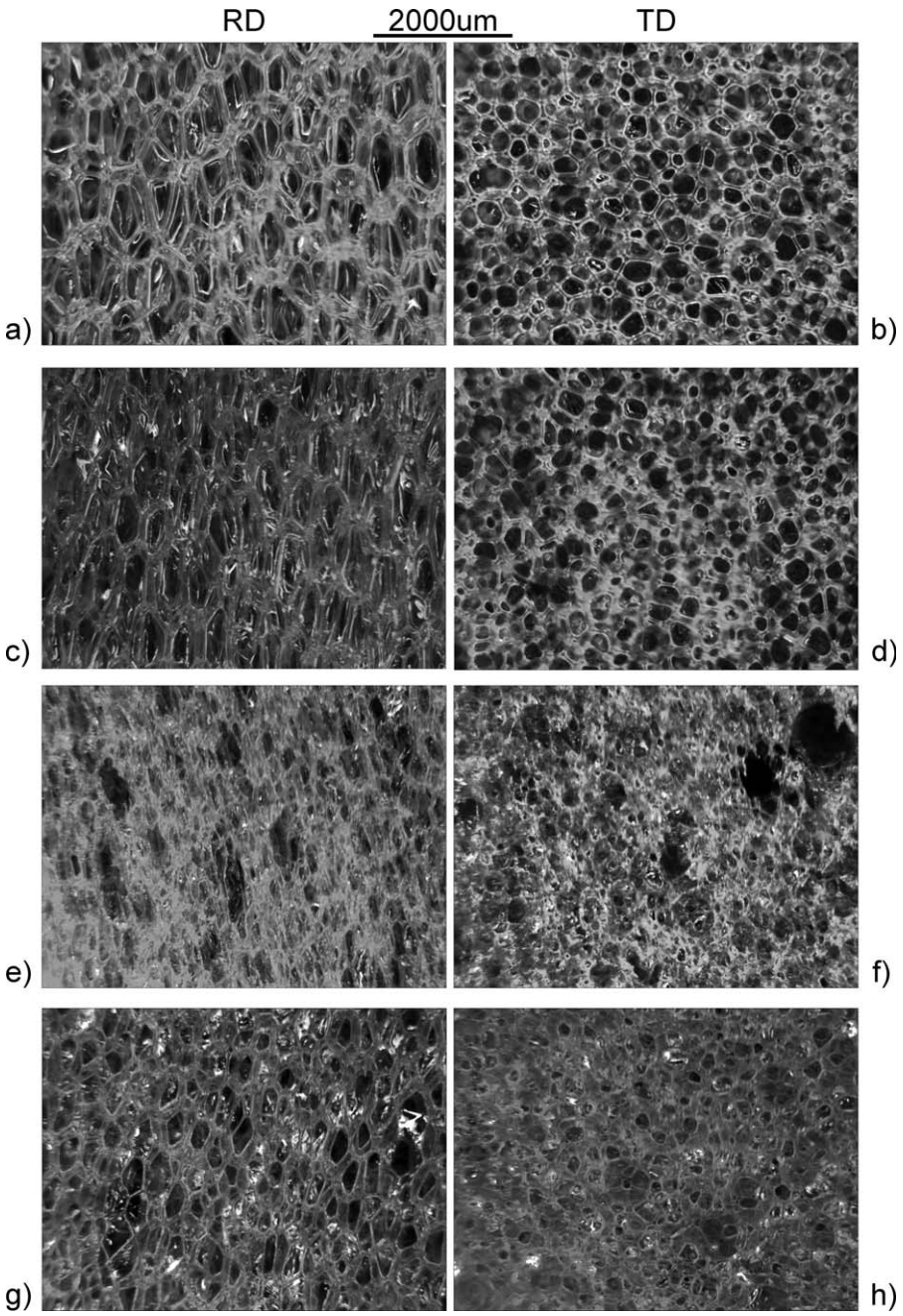

Figure 6. Optical micrographs of the foams (a,b) PPG-G; (c,d) PEG-G; (e,f) B90; (g,h) B130; in the rise and transverse directions, respectively.

within the range of 28–41 kg/m^3. From the literature, the behavior of polymeric foams within this density range tend to exhibit the following stages under compressive loading: (1) linear elasticity that corresponds to struts bending; (2) nonlinear elastic collapse that represents buckling of struts; (3) a plateau region of plastic collapse characterized by plastic hinging of struts; and lastly (4) densification, where a steep increase in stress occurs as the cellular material starts to resemble a solid material. Furthermore, with a large amount of closed cells the compression of the contained gas as well as membrane stretching can influence the stress-strain behavior.[39]

The lower density of the bark foam B130 possibly stems from small amounts of water in the polyol. PEG is a highly hydrophilic polymer; therefore maintaining low moisture content is more difficult than in a polypropylene oxide-based polymer. Regarding the modulus, both control foams had higher values than the bark foams. The elastic properties of PUFs are dependent on the closed-cell content. In an open-cell PUF, strut bending and cell wall axial deformation are the primary elastic deformation mechanisms. Whereas in a closed-cell PUF there are additional contributions from the cell membrane stretching and pressurization of the enclosed gas are also included.[39] Since

Table V. A Comparison of Compression Strength Data from Liquefied Biomass-Based Polyols and from Biomass-Polyol Blends

Biomass	Preparation of polyol	Isocyanate index	Density (kg/m^3)	σ_{10} (kPa)	Normalized strength $\sigma_{10}/\rho^{3/2}$ [kPa/(kg/m^3)$^{3/2}$]
Bark	Liquefaction	1.1	29–35	73–100	0.65
Bamboo[40]	Liquefaction	1.0	30–35	65	0.23[a]
Wood[41]	Liquefaction	1.2	35–37	70–106[b]	0.51[a]
Bark[44]	Blend	1.0	10–20	40	0.87[a]
Lignin/mollasses[42]	Blend	1.1	35–70	300–400[c]	0.99[a]
Lignin[43]	Blend	1.2	60–80	300–400[d]	0.62[a]

[a] Samples with the highest compression strength had their strength values extracted from graphs and then divided by their density. Variation was from changing the [b]liquefaction time; [c]lignin-molasses ratio; [d]mixing time and only PEG-based data was included.

the closed-cell content was much lower in the bark foams (Table IV), it corresponds that the modulus values were also lower. Some of the bark samples were nonlinear below 5 % strain. This could have been due to the uneven distribution of stress, caused by a higher frequency of defects and cell size heterogeneity. Cell heterogeneity would lead to stress concentration at large cells causing their long struts to buckle.

Stress values at both 10 and 25% strain were used to determine the specific compression strength of the PUFs. The specific compression strength is an ideal metric to compare foams since foam strength is proportional to $\rho^{3/2}$.[39] Thus, normalizing for density helps to facilitate a better comparison. B90 has the lowest specific compression strength of all foams, whereas B130 was equivalent to the PEG-G sample. Since compression testing was done in the rise direction, samples that were anisotropic and elongated in the rise direction would buckle more easily. Qualitatively from the optical images in Figure 6 it can be observed that PEG-G and PPG-G were more anisotropic than B130, and perhaps this was why B130 performed comparably well, despite having a low value for the closed-cell content and low density. In combination with the swelling, soluble fraction, and glass transition results it would appear that B90 likely had a less cohesive polymer network and poorer morphology compared to B130, and resulted in lower specific compression strength. It is likely that the higher liquefaction temperature of 130°C produced large condensation polymers that created a stable PU network earlier than the many smaller molecular weight chains in the lower liquefaction at 90°C. A more stable network would freeze the morphology and prevent the coalescence and Ostwald ripening of cells.

Comparisons to the literature can be difficult since researchers use different definitions of compression strength (the value at 10% will be used hence forth for comparison) and vastly different foam formulations. However, if the isocyanate index and density are similar a comparison may still provide some insight. From Table V it would appear that despite having liquefied polyols produced from vastly different biomass sources (bamboo[40]/wood[41]/bark) that bark and wood exhibited relatively similar compressive behavior. Measurements of closed-cell content were not available in the literature, but it was clear from this work that if the amount of closed-cell content were increased it would be an avenue to further enhance the properties of iquefied bark-based PUFs. PUFs produced from blending bark with a polyol resulted in a high normalized strength, primarily due to the very low density foams produced. The low density values reported may be due to rapid catalysis of the polyurethane reaction by using dibutyltin dilaurate as a catalyst. The work done by Hatakeyama et al.[42,43] presents foams with very high compression strengths. Since liquefaction and blending may be used together, this may be an approach to increase the compressive strength, while creating a polyol with even greater biomass content. To summarize, liquefied bark-based polyols have been shown to produce foams with higher normalized compression strength than other liquefied biomass-based polyols and with normalized compression strength within the range of PUFs based upon blends.

CONCLUSIONS

By systematically comparing bark foams to control foams the effect of liquefied bark content could be observed. The analysis of the foaming kinetics and thermal stability showed that the properties of the PUF are not negatively impacted by the presence of the bark compounds, but rather strongly related to the type of hydroxyls present and the total hydroxyl value. Analysis using DMA showed glass transition temperatures were within a comparable temperature range of 145–160°C. The bark foams exhibited less intense tan δ peaks, which implied the presence of high functionality compounds that enabled elastic behavior, but restricted viscous flow. The presence of liquefied bark compounds was found to cause a high amount of open-cell content. This is of importance since the modulus of both bark foams were lower than the controls and closed-cell content has a role in the elastic behavior due to membrane stretching and gas pressurization. This may have been due to the presence of low molecular weight compounds with low functionality, and resulted in unstable membranes that ruptured. The soluble fraction of the bark foams was also higher than the controls and confirms the presence of low functionality, low molecular weight compounds. Furthermore, bark foams have a less well defined morphology compared to the controls that indicated the bark polymers could have lower surface tension resulting in unstable cell growth and expansion or took longer to form a stable polymer network. These results show that in most aspects the presence of bark does not negatively impact the properties,

but on some foam characteristics like cell morphology and open-cell content it does exert an influence.

By comparing the two bark foams, B90 and B190, to each another the effect of liquefaction temperature on foam properties could be observed. The bark foam B130 that was produced at a higher temperature had a higher elastic modulus and higher compression strength, while at a lower foam density. The greater fraction of high molecular weight compounds, with likely greater functionality, was presumably the reason. In contrast, the P90 polyol used to produce the B90 foam had a large amount of small molecular weight compounds that proved to be deleterious to foam properties.

This research showed that liquefaction of bark can produce foams with similar characteristics to a control sample, has identified areas for optimization, and has shown that liquefaction temperature is a key determinant of foam characteristics. It is hoped that with continued research, the properties may be further improved and the viability of bark-based PUFs may come closer to fruition.

ACKNOWLEDGMENTS

The authors would like to acknowledge the financial support from the ORF-"Bark biorefinery" partners and FPInnovations for supplying lodgepole pine bark.

REFERENCES

1. Zhao, Y.; Yan, N.; Feng, M. W. *ACS Sustain. Chem. Eng.* **2013**, *1*, 91.
2. Zhao, W.; Pizzi, A.; Fierro, V.; Du, G.; Celzard, A. *Mater. Chem. Phys.* **2010**, *122*, 175.
3. Zhao, W.; Fierro, V.; Pizzi, A.; Du, G.; Celzard, A. *Mater. Chem. Phys.* **2010**, *123*, 210.
4. Lacoste, C.; Basso, M. C.; Pizzi, A.; Laborie, M.-P.; Celzard, A.; Fierro, V. *Ind. Crops Prod.* **2013**, *43*, 245.
5. Hartman, S. *Am. Chem. Soc.* **1977**, *43*, 257.
6. Ge, J. J.; Sakai, K. *Mokuzai Gakkaishi* **1993**, *39*, 801.
7. Zhao, Y.; Yan, N.; Feng, M. *J. Appl. Polym. Sci.* **2011**, *123*, 2849.
8. Ueno, T. *Mokuzai kogyo* **2007**, *62*, 358.
9. Gao, L.; Liu, Y.; Lei, H.; Peng, H.; Ruan, R. *J. Appl. Polym. Sci.* **2010**, *116*, 1694.
10. Jin, Y.; Ruan, X.; Cheng, X.; Lü, Q. *Bioresour. Technol.* **2011**, *102*, 3581.
11. Zheng, Z.; Pan, H.; Huang, Y.; Chung, Y. H.; Zhang, X.; Feng, H.; Service, U. F. *Open Mater. Sci. J.* **2011**, *5*, 1.
12. Kržan, A.; Žagar, E. *Bioresour. Technol.* **2009**, *100*, 3143.
13. Hu, S.; Wan, C.; Li, Y. *Bioresour. Technol.* **2012**, *103*, 227.
14. Wang, H.; Chen, H. Z. *J. Chin. Inst. Chem. Eng.* **2007**, *38*, 95.
15. Hakim, A. A. A.; Nassar, M.; Emam, A.; Sultan, M. *Mater. Chem. Phys.* **2011**, *129*, 301.
16. Ge, J.; Zhong, W.; Guo, Z.; Li, W.; Sakai, K. *J. Appl. Polym. Sci.* **2000**, *77*, 2575.
17. Smith, J. H. G.; Kozak, A. *For. Chron.* **1981**, *57*, 156.
18. Hon, D. N. S.; Shiraishi, N. Wood and Cellulosic Chemistry, 2nd ed.; Marcel Dekker Inc.: Basel, New York, **2001**; p 914.
19. Hirose, S.; Kobashigawa, K.; Izuta, Y.; Hatakeyama, H. *Polym. Int.* **1998**, *47*, 247.
20. Chattopadhyay, D. K. K.; Webster, D. C. *Prog. Polym. Sci.* **2009**, *34*, 1068.
21. D'Souza, J.; Yan, N. *ACS Sustain. Chem. Eng.* **2013**, *1*, 534.
22. Jasiukaitytė, E.; Kunaver, M.; Crestini, C. *Catal. Today* **2010**, *156*, 23.
23. Campanella, A.; Bonnaillie, L. M.; Wool, R. P. *J. Appl. Polym. Sci.* **2009**, *112*, 2567.
24. Cateto, C. A. A.; Barreiro, M. F. F.; Rodrigues, A. E. E. *Ind. Crops Prod.* **2008**, *27*, 168.
25. Romero, R. R.; Grigsby, R. A.; Rister, E. L.; Pratt, J. K.; Ridgway, D. *J. Cell. Plast.* **2005**, *41*, 339.
26. Richter, E. B.; Macosko, C. W. *Polym. Eng. Sci.* **1978**, *18*, 1012.
27. Torres-Sánchez, C.; Corney, J. *J. Polym. Res.* **2008**, *16*, 461.
28. Entelis, S. G.; Nesterov, O. V. *Russ. Chem. Rev.* **1966**, *35*, 917.
29. Rand, L.; Thir, B.; Reegen, S. L.; Frisch, K. C. *J. Appl. Polym. Sci.* **1965**, *9*, 1787.
30. Coates, J. Encyclopedia of Analytical Chemistry; Wiley: Chichester, London, **2000**.
31. Bhattacharjee, D.; Engineer, R. *J. Cell. Plast.* **1996**, *32*, 260.
32. Gaboriaud, F.; Vantelon, J. P. *J. Polym. Sci.* **1982**, *20*, 2063.
33. Hatakeyama, H.; Marusawa, T.; Hatakeyama, T. *J. Mater. Sci.* **2011**, *46*, 7475.
34. Ravey, M.; Pearce, E. M. *J. Appl. Polym. Sci.* **1997**, *63*, 47.
35. Wang, T.-L.; Hsieh, T.-H. *Polym. Degrad. Stab.* **1997**, *55*, 95.
36. Wu, L.; Gemert, J. Van; Camargo, R. E. *Proc. CPI Polyurethanes Tech. Conf.* **2008**, 1.
37. Rhodes, M. B. In Polymeric Foams Science and Technology; Khemani, K. C., Ed.; American Chemical Society: Washington, DC, USA, **1997**; p 178.
38. Saunders, J. H.; Frisch, K. C. Polyurethanes Chemistry and Technology Part 1. Chemistry; Wiley: New York, London, Sydney, **1962**; p 368.
39. Gibson, L. J.; Ashby, M. F. Cellular Solids Structure and Properties; 2nd ed.; Cambridge University Press: Cambridge, **2001**; p 510.
40. Gao, L.; Liu, Y.; Lei, H.; Peng, H.; Ruan, R. *J. Appl. Polym. Sci.* **2010**, *116*, 1694.
41. Zheng, Z. F.; Pan, H.; Huang, Y. B.; Chung, Y. H. *Adv. Mater. Res.* **2010**, *168*, 1281.
42. Hatakeyama, H.; Kosugi, R.; Hatakeyama, T. *J. Therm. Anal. Calorim.* **2008**, *92*, 419.
43. Hatakeyama, H.; Hirogaki, A.; Matsumura, H.; Hatakeyama, T. *J. Therm. Anal. Calorim.* **2013**, *114*, 1075.
44. Nakashima, Y.; Ge, J. J.; Sakai, K. *Mokuzai Gakkaishi* **1996**, *42*, 1105.